Neural, Parallel, and Scientific Computations 28 (2020) 53-71

Fault Diagnosis in Wind Turbine Planetary Gearbox Using Vibration Time-Frequency Analysis Technique

Shawki A. Abouel-Seoud[1],Mohamed M. Abdel-hafiz[1*], Ahmed S. Abdallah[1], Mohamed N. Mansy[1]
[1]Faculty of Engineering (Mataria), Helwan University, Masaken El helmia P.O.Box 11718, Cairo Egypt
[*]Corresponding author: dr.mohamed.hafiz@m-eng.helwan.edu.eg

Abstract

Fault diagnosis for wind turbine planetary gearboxes is an important task for reducing their maintenance cost. In this paper, a method for the trouble diagnosis of the wind turbine gearbox, planet gear and faults is proposed, where the vibration signature was applied in which the time-frequency analysis technique such as continuous wavelet transformation was employed. A test rig was set up to simulate the working of a wind turbine planetary gearbox. The faults considered are tooth crack, tooth spalling and tooth breakage which was tested under accelerated fault conditions where the filtering process of the time signals was applied to the vibrations of gears to indicate the existence and develop of the fault. The indicator of the diagnostic technique; namely spectral kurtosis is used for the filtered vibration signals. The results demonstrate that the proposed technique has a good de-noising overall performance and is located to be very effective in the detection of signs and symptoms from vibration alerts of a gearbox with early tooth faults.

Keywords: Wind turbine, Planetary gearbox, Vibration signature, Gear fault diagnosis, crack inspection, breakage

1. Introduction

Wind turbine planetary gearboxes regularly run underneath nonstationary situations because of unstable wind situations, as a consequence ensuing in nonstationary vibration signals. Time-frequency evaluation gives insight into the shape of an arbitrary nonstationary signal in joint time-frequency domain, however traditional time-frequency representations be afflicted by both time-frequency smearing or cross-term interferences. Reassigned wavelet scalogram has deserves of best time-frequency decision and cross-time period free nature however has very restricted applications in equipment fault discover. However, reassigned wavelet scalogram to extract fault characteristic from wind turbine planetary gearbox vibration indicators has been utilized.

The dynamic behaviors of established' machines in All most manufacturing web sites commonly fluctuate because of different in their foundation flexibilities, which is possibly why separate analysis become regularly required for each machine for the duration of fault diagnosis. In practice, the fault diagnosis technique is even in addition complex by the truth that evaluation become regularly carried out at individual measurement locations for variable speeds, because a large number of rotating machines work at various speeds. consequently, via the experimental simulation of a comparable practical situation of identically configured 'as established' rotating machines with variable foundation flexibilities, this survey proposes A simplified vibration- based fault diagnosis experimental rigs with variable basis flexibilities, many of common rotor-associated faults had been independently. Records mixture method was then used for computing composite better method has been proposed that can be precious for fault detection regardless of basis flexibilities or running speeds (Kaltungo, et al 2015; Lei, et al, 2013).On both order spectra (composite bi-spectrum and com spectrum), teeth and a missing tooth are carried out. And the vibration signals had been gathered under the loaded situation and different motor speeds.

In sign processing applications, it is regularly important to extract oscillatory components and their properties from time-frequency representations, e.g. the windowed Fourier transform, or wavelet transform. step one on this process became to discover the correct ridge curve: a sequence of amplitude height positions (ridge points), corresponding to the component of interest and supplying a measure of its immediately frequency. This isn't a trivial problem, and the optimal technique for extraction was still no longer settled or agreed. processes which may be used for this mission and evaluate their overall performance on both simulated and actual data have been discussed and developed particularly, a

Received March 1, 2020
www.dynamicpublishers.org

https://doi.org/10.46719/NPSC20202814

technique has been proposed which, in contrast to many different processes, became highly adaptive in order that it did not want any parameter adjustment for the signal to be analyzed (Iatsenko, et al, 2013). Being primarily based on dynamic direction optimization and stuck point generation, the technique became very rapid, and its superior accuracy became also verified. in addition, the benefits have been investigated and draw backs that synchro squeezing gives on the subject of curve extraction.

Because of the individual of variety and complexity, the compound faults detection of rotating machinery under non-stationary operation will become a challenging mission. Multiwavelet with or extra base functions and lots of great properties presents an opportunity to discover and extract all of the functions of compound faults at one time. but, the constant basis features independent of the vibration signal can also decrease the accuracy of fault detection. Furthermore, the decomposition results of discrete multiwavelet transform does no longer possess time invariance, which became harmful to extract the function of periodical impulses (Chen, et al, 2013). to conquer these deficiencies, based totally at the Hermite splines interpolation, taking the minimum envelope spectrum entropy as the optimization goal, adaptive redundant lifting multiwavelet became advanced. Additionally, to be able to remove errors propagation of decomposition results, adaptive redundant lifting multiwavelet became improved via adding the normalization factors. As an effective technique, Hilbert transform demodulation evaluation became used to extract the fault function from the excessive frequency modulation signal. The proposed technique incorporating advanced adaptive redundant lifting multiwavelet (IARLM) with Hilbert transform demodulation evaluation became carried out to compound faults detection for the simulation experiment, rolling element bearing check bench and journeying unit of electrical locomotive.

These days, Wavelet transform (WT) has been verified to be greater suitable for evaluation of vibration signals, because maximum of the time-vibration signals have immediately impulse trains and show off a transient (non-stationary) nature. An adaptive wavelet filter out has been used, based totally at the Morley wavelet, carried out at the torsional vibration data measured from a single-stage gearbox with artificially caused cracks inside the gear. This was completed to extract a few parameters and test their diagnostic conduct to be able to look for those with the most potential and appropriateness for future health monitoring schemes (Morsy, et al. 2011). It became determined to be very powerful in detection of signs and symptoms from vibration signals of a gearbox with early tooth cracks. Furthermore, the effects of crack intensity, velocity and load at the wavelet entropy have been introduced. Multi-hour tests had been carried out and recordings had been obtained the use of torsional vibration monitoring. Similarly, the transitions inside the wavelet entropy values with the recording time have been highlighted suggesting important modifications in the operation of the gearbox
Early bearing fault diagnosis techniques normally take time–frequency evaluation as the essential basis, for looking via characteristic fault frequencies based totally on bearing kinematics to discover fault places. But, because of mode mixing, the characteristic frequencies have been commonly masked by using normal frequencies and therefore had been hard to extract. After time–frequency decomposition, the effect signal frequency may be disbursed amongst multiple separation functions consistent with the mode mixing as a result of the effect signal; consequently, it became feasible to look for the shared frequency top value in those separation functions to diagnose bearing faults. The use of the wavelet transforms, time–frequency evaluation and blind supply separation principle, a new technique of determining shared frequencies were supplied (Cui, et al, 2017) observed via identifying the defective elements of bearings. Compared to rapid independent factor evaluation, the sparse element analysis became better capable of extract fault characteristics. The numerical simulation and the practical utility test received excellent results while combining the wavelet transform, intrinsic time-scale decomposition and linear clustering sparse element evaluation, thereby proving the validity of this technique.

A technique for category of mammographic loads as benign or malign has investigated, where the examine relies on a mixture of support Vector machine (SVM) and wavelet-based totally sub-band image decomposition. Decision making became performed in stages as feature extraction via computing the wavelet coefficients and class the usage of the classifier skilled at the extracted functions. SVM, a studying system based on statistical studying principle, became trained thru supervised studying to classify masses, where sixty-six digitized mammographic images concerned. The masses have been segmented manually via radiologists, prior to introduction to the class system (Gorgei, et. al 2009, Abouel-seoud, 2018). Initial test on mammogram confirmed over 84.8% classification accuracy using the SVM with Radial basis function (RBF) kernel. Additionally, confusion matrix, accuracy, sensitivity and specificity evaluation with variable kernel kinds had been used to expose the classification overall performance of SVM.

To deal with the shortage of powerful experimental statistics under the present-day situation for gearbox fault sample popularity, the Wind Turbine Drivetrain Diagnostics Simulator (WTDS) became used for experimental investigation and received huge quantity of gear fault samples. The wavelet transform became hired to decompose the vibration signal to achieve the power ratio in every frequency band. Taking energy ratios as feature vectors, the sample recognition results have been received via the support vector

class (SVC) (Li, and Xiang, 2014, Entezami and Shariatmadar 2018). The experimental results of hybrid technique display that become strong to noise and has excessive category accuracy.

The above referred to works have shown that the vibration-based totally tools diagnostics has been the most famous monitoring method due to its excessive effectiveness. furthermore, the wavelet transform (WT) is widely used within the sign de-noising manner wavelet analysis, where it's miles the most popular method for analyzing the non-desk bound signals and overcomes the drawbacks of different strategies with the aid of analytical features which are neighborhood in each time and frequency but, the focal point of this take a look at is to rent the vibration records gathered from the simulated wind turbine planetary gearbox planet gear at speed of 20 rpm, 20 Nm and forty rpm, 40 Nm take a look at conditions to perform the fault diagnostic methods, wherein the vibration evaluation was carried out in which the time-frequency evaluation method such as continuous wavelet transformation (CWT) turned into employed. And applied at the rotational vibration statistics measured with artificially induced crack, spalling and breakage in the planet tools enamel. That is accomplished to permit the vain noise in raw vibration alerts to be filtered. Moreover, ordinal ranking was applied to diagnose the planet tools for one of a kind faults in addition to the severity of the fault and associated problems and assessing of the contemporary healthy condition are discussed.

2. Wind turbine gearbox non-stationary operating conditions

Problems in wind turbine gearbox diagnosis come from no longer only the complexity of the structure (e.g., the difficulties as a result of the planetary stage), however additionally the instability of operation situation. Signal evaluation of gearbox in nonstationary operations can be very extraordinary from the stationary operations. The load and velocity of gearbox varies over time because of the randomness of the wind, which causes apparent non-stationarity in vibration reaction. Therefore, it is a difficult issue to discover failures over the time-varying non-stationary operation. It is crucial to become aware of the external varying load situations for condition monitoring of planetary gearboxes for the reason that vibration reaction is susceptive to load.

The area of expertise in wind turbine gearbox and the nonstationary operation situations result in the demanding situations in signal evaluation. Furthermore, some crucial fault features are buried in noises, in order that we cannot come across the failures efficiently. For that reason, the perfect technique for susceptible characteristic extraction is big to fault detection. Approaches for vulnerable feature extraction can be divided into two categories: statistical strategies (wavelet related methods, singular price decomposition, stochastic resonance, and many others.), and artificial intelligence (AI) methods (neural networks, genetic algorithms, and so on.). Vibration-based totally condition monitoring (VCM) is the most famous and acknowledged CM technique, especially for gearboxes, as within the observe of. (Márquez et al, 2012). It is accomplished with the aid of measuring vibrations of the components in actual time to detect adjustments in the dynamic behavior of the tool.

3. The Continuous Wavelet Transform

3.1. Definition

Wavelet transforms are internal products among signals and the wavelet own family, which might be derived from the mom wavelet through dilation (scale) and translation. Allow g (t) be the mother wavelet, the daughter wavelet will be g a,b(t) = g ((t – b)/a), where a is the scale parameter and b is the time translation. Through varying the parameters a and b, one of a kind daughter wavelets may be acquired that represent a wavelet own family. Wavelet remodel is to carry out the subsequent operation (Kaltungo, et al 2015).

$$W_g(a;b) = \frac{1}{\sqrt{a}} \int_{-\infty}^{+\infty} x(t) \psi * g^* dt \quad \textbf{(1)}$$

Where: Wg (a,b) is the function after transformed, andg * (t) stands for complex conjugation of g (t). For the function g (t) to qualify as an analyzing wavelet, it must satisfy the admissibility conditions

$$C_q = \int_{-\infty}^{+\infty} \frac{|G(\omega)|}{|\omega|} \quad \textbf{(2)}$$

where G(ω) is Fourier transform of g (t). This is needed in obtaining the inverse of the wavelet transform.

If a daughter wavelet is considered as a filter, wavelet transform is certainly a filtering operation. normally, reconstructing the wavelet coefficients at decided on scales via sure techniques attempted to be located. To do that, prior data needed to be recognized on the sign wishes to be recognized.

3.2. Morlet Wavelet Filter

The continuous wavelet transform (CWT) is used to obtain the wavelet coefficients of signals. The statistical parameters of the wavelet coefficients are extracted which constitute the feature vectors. The Morlet wavelet is one of the most popular non-orthogonal wavelets, the definition of Morlet is:

$$\psi(t) = \exp\left(-\frac{\beta^2 t^2}{2}\right)\cos(\pi t) \quad \textbf{(3)}$$

It is a cosine signal that decays exponentially on both the left and right sides. This feature seems very similar to an impulse. It has been used for impulse isolation and mechanical fault diagnosis through the performance of a wavelet De-noising procedure. However, in practice, it is not easy to provide a proper threshold for wavelet de-noising. This is can be avoided by using an adaptive wavelet filter instead of wavelet denoising

3.3. Adaptive Morlet Wavelet Filter

A daughter Morlet wavelet is obtained by time translation and scale dilation from the mother wavelet, as described in the following formula[Márquez et al, 2012).

$$\psi_{a,b}(t) = \psi\left(\frac{t-b}{a}\right) = \exp\left[-\frac{\beta^2 (t-b)^2}{2a^2}\right]\cos\left[\frac{\pi(t-b)}{a}\right] \quad (4)$$

Where (a) is the scale parameter for dilation and (b) is the time translation. it may additionally be checked out as a filter. To pick out the immersed impulses through filtering, the place and the form of the frequency band similar to the impulses ought to be determined first. Scale (a) and parameter (β) manage the area and the form of the daughter Morlet wavelet respectively. As a result, an adaptive wavelet filter out might be constructed with the aid of optimizing the 2 parameters for a daughter wavelet. Several researchers have reported on a way to choose a mother wavelet that adapts the first-class to the sign to be isolated. The method of (β) selection in a Morlet wavelet is primarily based on maximum Kurtosis. Details of how to pick (β) and (a) in a Morlet wavelet based totally on Kurtosis to make the mother wavelet suit the signal to be isolated had been supplied in (Morsy, et al 2010). on this analysis, awareness has been located on finding the first-rate wavelet clear out (the daughter wavelet of a Morlet wavelet) in preference to optimal wavelet reconstruction.

3.4. The Spectral Kurtosis

Some of statistical measures can then be used at the demodulated signal as an indicator at the existence and status of gear fault. in the present work, the present day techniques are used for detecting and diagnosing localized gear faults under extraordinary operation conditions, and as compared with current gear diagnostic techniques. The fault in rotating system including a neighborhood equipment fault introduces periodic impacts that seem as impulse-like peaks inside the measurements. The kurtosis (Kurt) is utilized in engineering for detection of fault signs and symptoms because it is sensitive to sharp variant systems, such as impulses (Sharma and Parey 2015). The larger impulse in signals indicates the bigger kurt. As an end result, kurt may be used because the overall performance measure of a Morlet wavelet clear out. Even though, an excessive kurtosis value for a given statistics set indicates a presence of a distinct height; but, kurt fee decreases when the measured information set consists of periodic impulses repeating at the period of a fault. The Kurt is simply the normalized fourth moment of the sign. The instant is normalized to the square of the variance of the sign. The kurtosis is a statistical measure of the number and amplitude of peaks in a signal. This is, a signal that has greater and sharper peaks will have a bigger value, the definition of Kurt is:

$$Kurt(x) = E(x^4) - 3.[E(x^2)]^2 \quad \textbf{(5)}$$

Where x is the sampled time series, E represents the mathematical expectation of the series and Kurt (x) is Kurt of the signal.

3.5. Faults Severity Assessment

From the previous discussion, descriptive and higher order statistics (HOS) indices have been generating intensive interest. The kurtosis (kurt) values for filtered signal calculated from the measured signal is found to be a better indicator as compared with the other. However, the kurt values of rotational vibration acceleration is used to evaluate the wind turbine gearbox components faults severity assessment. Component fault health level (CFHL) can be calculated based on the following equation

$$CFHL,(\%) = \frac{(KT)_{Faulty} - (KT)_{Healthyy}}{(KT)_{Healthyy}} \quad \textbf{(6)}$$

Where

$CFHL,(\%)$ = Component fault health level

$(KT)_{Healthy}$ = Kurtosis value for healthy condition

$(KT)_{Faulty}$= Kurtosis value for faulty condition

4. GEARBOX TEST RIG ESTABLISHMENT

4.1. Background

The gearbox is located inside the nacelle, and it is one of the important components of the drive train. Fig. 1 indicates an ordinary configuration of a wind turbine drive train, with the gearbox positioned among the rotor and the generator. Aside from the gearbox, other applicable sub-systems are included inside the drive train, which engage with the gearbox and might make contributions to its failures: Bearings the main function of bearings is lowering frictional resistance among two surfaces with relative movement, both linear and rotational. According to the kind of motion, bearings are divided in two classes: linear/axial and rotational/radial bearings. An axial bearing is employed inside the main shaft, even as radial bearings are specifically used for the gears and the main bearing. Bearings are in lots of cases liable for gearbox failures (Musial, et al, 2007).

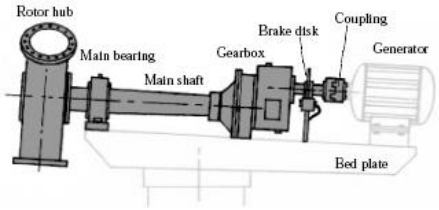

Fig. 1 Typical drive train of a wind turbine (reproduced by (Musial, et al, 2007)

4.2. The Wind Turbine Gearbox

The wind turbine gearbox is located among the master shaft and the generator, its mission is to growth the slow rotational velocity of the rotor blades to the generator rotation velocity of 1000 or 1500 revolutions in step with minute (rpm). Without lots preceding experience with wind turbines, one would possibly assume that the gearbox might be used to alternate speed, similar to an ordinary automobile gearbox. But this isn't always the case with a gearbox in a wind turbine. In this situation the gearbox has usually a consistent and a velocity growing ratio, in order that if a wind turbine has different operational speeds, it is because it has two unlike sized generators, each with its very own extraordinary speed of rotation (or one generator with two unlike stator windings).

for example, a wind turbine gearbox has 3-stage, wherein the primary stage is planetary and the second one and third degrees are helical, the distinction inside the size of the wheels is identical or over 1:5 inside the first stage, even as the difference in size of the wheels is also same or over 1:5 inside the second and third degrees. While the two ratios are mixed, the output shaft will flip 25 times for each rotation of the whole shaft (input) and the master shaft of the wind turbine combined. You'll say that the equipment container has a gear ratio of 1:25. Commonly the ratio in each set of gearwheels is restrained to approximately less than 1:6. If the a hundred and fifty kW wind turbine has a rotor rotational velocity of forty rpm and with a generator pace of approximately a thousand rpm, the gearbox ought to have a complete equipment ratio of forty/1000 or 1:25. This is possible the use of a three-stage gearbox (one planetary stage and the other represents the double helical stages connecting via flexible coupling as seen in Fig. 2

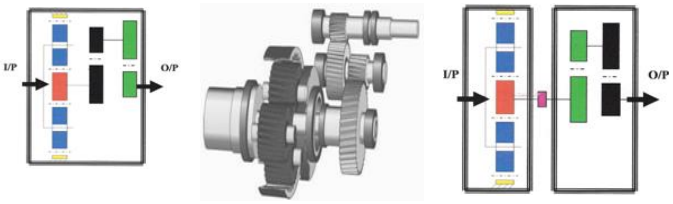

a) Real layout b) Real original c) Simulated layout

Fig. 2 *Wind turbine gearbox [Stiesdal, H. 1999]*

4.3. Experimental Simulation Set Up

Figures three and four display schematically arrangement format of test rig components and Accelerometers positions respectively the tested wind turbine gearbox is similar to the one described above (it includes 3 stages), where the primary stage is planetary and the second one and the third one stages are helical. Because of the difficulties to gain a actual gearbox in a single unit, consequently two separate units are considered, one planetary gearbox and the other is helical ge d helical) are linked via flexible coupling produce one combined g f planetary gearbox or helical gearbox are supported by using two bea x and the helical gearbox device is settled in an oil basin to be able to E ninety oil was used as a lubricant and the total lubrication level is o n level is 50 mm. The combined gearbox is powered through an ele s power on a hydraulic disc brake. A short shaft is connected direct o decrease outcomes of misalignment and transmission of vibration t its ends via bearings and then the movement is transmitted di n characteristics are as follows:

- 1-stage planetary gearbox with 3 planet gears
- 2-stage helical gearbox with 4 helical gears
- 3-phase 11 kW motor (220 V, 50 Hz, 1440 rpm) managed through an inverter
    - Hydraulic disc brake
    - The shafts are bearing supported.

Because the planetary stage has an excessive torque with low velocity and consequently most of the failure modes occur on this stage, consequently, all of the experimental work can be finished at the planetary stage rather than at the helical stages.

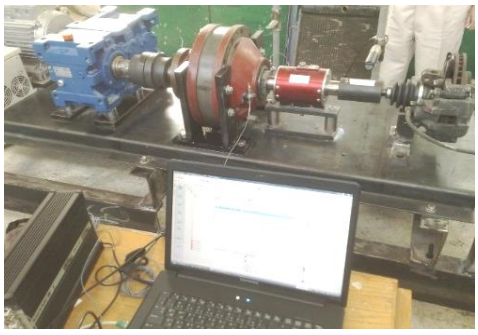

Figure 3 The real photo of arrangement

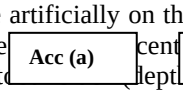

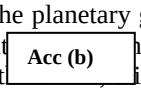

Figure 4 Accelerometers positions

4.4. Description of the Artificial Fault

The planet gear in its healthy condition is shown in Fig.5, where the three small faultswhich have been made artificially on the planetary gearbox planet gear tooth, with wire electrical discharge machining to create cent eventually led to a propagating fault. The faults dimensions are: planet gear t lept ickness 0.2 mm), planet gear tooth spalling (length 0.9 mm, height =1.0 mm, width 4.6 mm) and planet gear tooth breakage (thickness 0.6 mm, height = 1.35 mm, width 4.6 mm); and are shown in Figs.5-8. For each defect, a recordings every 15 min were acquired and a total of 12 recordings (0-3 hr of test duration) were resulted until the termination of the test. This type of test was preferred in order to have the opportunity to monitor path defect modes, i.e., the natural defect propagation.

Fault is assured by increasing the test period to the point of where the remaining metal in the tooth area has enough stress to be in the plastic deformation region.

5. Test Procedure

The complete turbine gearbox (planetary and helical) is driven at a fixed input velocity using a 15 horsepower (hp), 1440 rev/min AC power motor. The maximum velocity and load are 40 rev/min and 15 Hp. the velocity range will be carried out by using varying the frequency to the motor with an AC inverter unit. The mechanical and electr losses are sustained via a small fraction of complete electricity. The set up test rig has the capability of checking out most of wind turbine gearboxes with ratios from approximately 25 to 50. The system is sized to offer the most versatility to velocity and load settings. The use of various velocity ratios and gearboxes than indexed on this study is viable if suitable consideration to system operation is given. The motor, hydraulic disc brake, flywheel and gearbox are difficult-set up and aligned on a bedplate. The bedplate is established by using isolation feet to prevent vibration transmission to the ground. The shafts are linked with each flexible and inflexible couplings. it is widely known that most of the motions inside the gearbox are rotational. but, it is extremely uncommon to find sufficient references and techniques for the measurement of rotational responses (displacement, velocity and acceleration) and this displays the reality that virtually none are made. this case arises from a large difficulty that is encountered when looking to measure both rotational responses or excitations and additionally when looking to apply rotational excitation, i.e., an excitation torque. This reflects the fact that virtually none are made, and because of this, two accelerometers were used to measure the translation vibration responses, from which the rotational vibration was predicted, based on the concept presented in [Ewins, 1986]. The distance between the positions of the accelerometers is considered as small as possible to prevent the influences of the flexibility on their reading (150 mm).One non-destructive technique has been employed to record the gearbox during operation, namely vibration acceleration generation. Two Bruel & Kjaer accelerometers Type4514B-001 were used for the vibration acceleration signals record. The signal was processed with a low pass anti-aliasing filter to eliminate signals above 2.0 kHz, in order to retain waveform integrity as much as possible. A number of 2048 samples were acquired in the experiments. This is corresponding to a time history length of 1.0 s. To analyze the results, a Bruel & Kjaer portable, multi-channel PULSE, Type 3560-B-X05 Analyzer and the measurement software Type 7700 were used. Also, a tachometer Type MM360 is used to measure the speed.

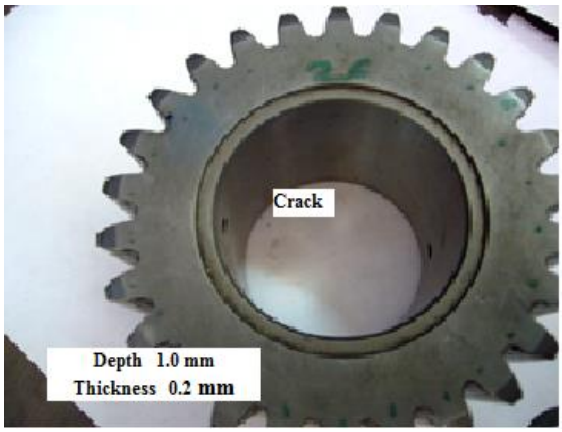

Fig.5Wind turbine planetary gearbox healthy components ***Fig.6*** *Wind turbine planetary gearbox Planet gear tooth crake*

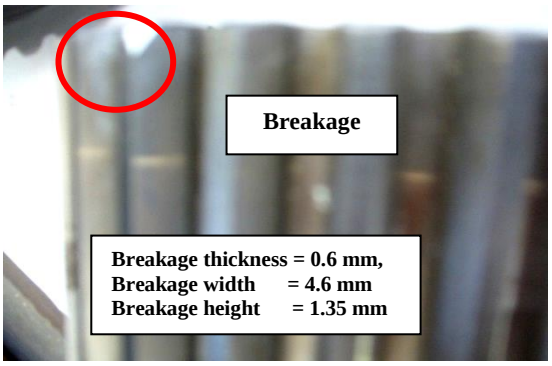

Fig. 7 *Wind turbine planetary gearbox: planet gear spalling tooth breakage*

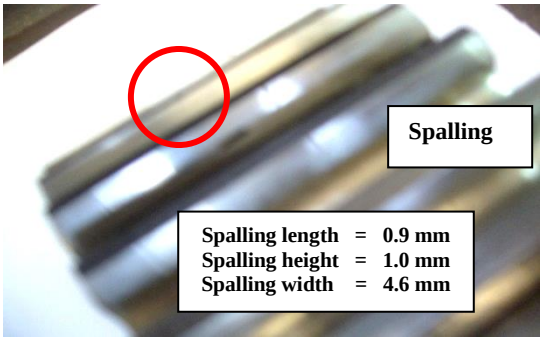

Fig. 8 *Wind turbine planetary gearbox planet gear tooth*

6. RESULTS AND DISCUSSION

6.1. Baseline Signal Analysis (Healthy)

In baseline case, all gears are healthful gearbox, where Figs. 9-10 exhibit the wavelet of the waveform signals for healthful gearbox components of rotational vibration acceleration in phrases of time-domain at velocity 20 rpm and torque load 20 Nm; and at velocity 40 rpm and torque load 40 Nm respectively. Figs. 9(a) and 10(a) display the experimental time domain signal at velocity 20 rpm and torque load 20 Nm and at velocity 40 rpm and torque load 40 Nm respectively, even as Figs. 9(b) and 10(b) display the reassigned wavelet scalogram (maps) of the baseline signal. It actually shows that the constituent time-domain components and their variations with the time, in which the distortion in color is almost repeated both 600 (40 rpm 40 Nm) and 1200 (20 rpm, 20 Nm) samples. Furthermore, the vertical axes represent the levels, even as the darker color shows higher energy. For this reason, the presence of those time-domain components does no longer mean the planet gear fault.

Only some weak components are seen, displaying that the gearbox is healthful, that is consistent with the experimental setting. Be aware that the wavelet maps display the relative magnitude of energy for each level. In other words, the relative magnitude is meaningful only for the cells in the identical degree, not throughout variable ranges. As soon as the time collection data has been converted to wavelet coefficients, the reference peak is positioned in each of the period and the periods are synchronously organized based totally at the 'book-marked' reference peak. Sample points can be dropped from the start or end of the periods which have extra sample points than the other periods. Despite the fact that losing the more sample points could introduce errors inside the analysis, this error may be considered to be insignificant if the records data acquisition rate is quite excessive.

Local faults in a gearbox are normally diagnosed by using detecting the presence of higher impulses inside the vibration signals. Although there may be no fault (healthful gearbox), tooth contact might also occur prematurely on the tip of the sun gear because of tooth deflection and the rate mismatch among the planet - sun gear and planet-ring gear. For the reason that an actual impulse is normally asymmetric, the right-hand side of the Morlet wavelet (Equation (3)) has been selected for use as the basis. Such wavelets need to match the behaviors of hidden impulses the best. Those purpose the impact on the time of contact which offers rise to the larger vibration on the planet gear meshing frequency. Consider the case of 20 rpm, 20 Nm, the filtering results with the Morlet optimized wavelet filter ($\beta = 1.2$ and $a = 6$) based totally on Equation (4). Periodic impulses are obvious in Fig. 9(b). because the velocity is 20 rpm, the time considered in the measurements is 1000 ms (1.0 s) and the planet gear teeth number is 26 teeth, then the periodic is equal to 1 divided by velocity (c/s) and is just about 3.0 s, even as the meshing frequency is calculated as gear teeth number divided via periodic and is equal to 8.665 Hz. With appreciate the case of 40 rpm, 40 Nm, the filtering results with the Morlet optimized wavelet filter ($\beta = 0.4$ and a = eight) based totally on Eq. (4). Periodic impulses are apparent in Fig. 10(b). because the velocity is 40 rpm, the time taken into consideration in the measurements is 1000 ms (1.0 s) and the planet gear teeth number is 26 teeth, then the periodic is equal to 1 divided by using velocity (c/s) and is just about 1.5 s, even as the meshing frequency is calculated as gear teeth number divided by using periodic and is equal to 17.33 Hz. it is understood that the gearbox is basically accelerated by using the force due to the tooth mesh, because the positions of the peak intensity nearly correspond to the beginning positions of tooth mesh, while inside the wavelet map, it is understood that the value of the component to meshing frequency is bigger than the other ones and varies with the development of the tooth mesh. Referring to Figs.9(a) and 10(a), the spectral kurtosis (kurt) values are computing based on Equation (5) and are3.07 rad/s^2 (20 rpm, 20 Nm) and 13.12 rad/s^2 (40 rpm, 40 Nm) respectively. On the other hand, it is well known that the normal distribution for the kurt is 3. This

indicates the good condition of the planetary gearbox components. However, the significant change around this number indicates the deterioration in condition.

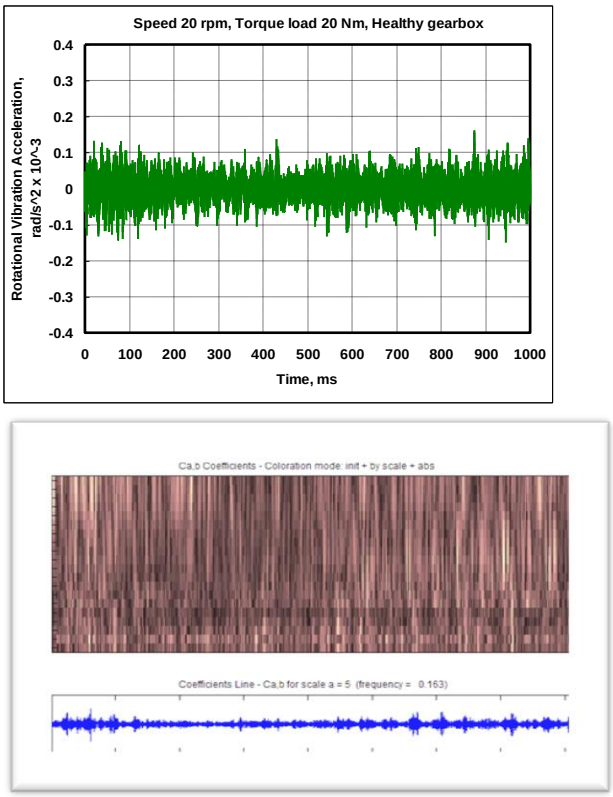

a) Experimental time-domain signal b) Signal wavelet map

beta =1.2, scale =6

Fig. 9 Wavelet-healthy gearbox of rotational vibration acc (20 rpm, 20 Nm)

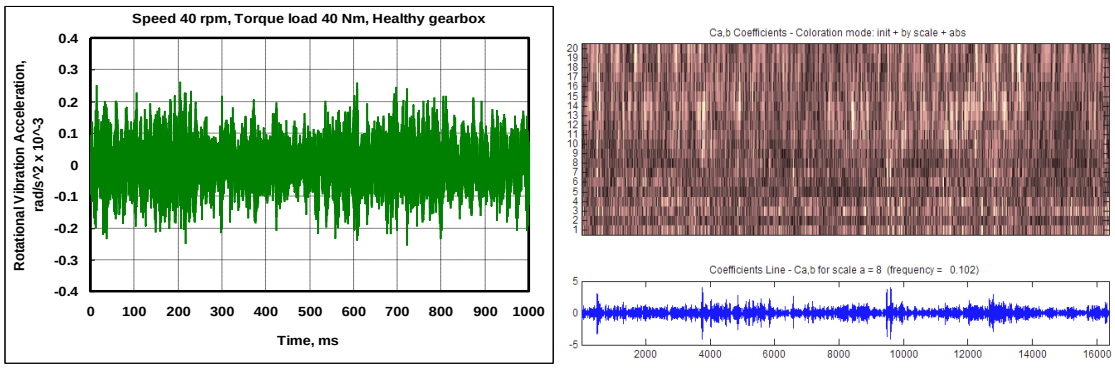

(a) Experimental time-domain signal b) Signal wavelet map

beta =0.4, scale =8

Fig.10 Wavelet-healthy gearbox of rotational vibration acc. (40 rpm, 40Nm)

6.2. Cracked Planet Gear Signal Analysis

Figures 11and 12 depict the signal measured for faulty (cracked cracked) planet gear tooth in terms of time-domain waveform at speed 20 rpm and torque load 20 Nm; and at speed 40 rpm and torque load 40 Nm respectively.Figures11(a) and 12(a) show the experimental time domain signal at speed 20 rpm and torque load 20 Nm and at speed 40 rpm and torque load; 40 Nm respectively, while Figs.11(b) and 12(b) show the wavelet maps where the distortion in color is nearly repeated each 1200 (20 rpm, 20 Nm) and 600 (40 rpm 40 Nm) samples. A close look at the vibration signal close to the gear meshing frequency reveals the presence of existing fault (crack) in the gears of the gearbox.

Based on the results shown in the figures, the crack is simplified and considered the crack path to be a straight line. The intersection angle between the crack and the central line of the tooth is set at a constant 45°. The crack depth is 1.0 mm and thickness 0.2 mm. The testing time is being 3.0 h. It can be seen that the planet gear tooth fault usually exhibits weak symptom in the vibration signal, because the planet gear is relatively far from the accelerometer mounted on the gearbox casing. But the time-varying planet gear fault characteristics are still identified, owing to the fine time-frequency resolution and capability in suppressing cross-term interferences of reassigned scalogram. This shows its effectiveness in extracting planetary gearbox fault features under nonstationary conditions. In spite of the uncertainly and the significant fluctuations, the kurtosis parameter is monotonically
y increased, which is very useful from a diagnostic
point of view.

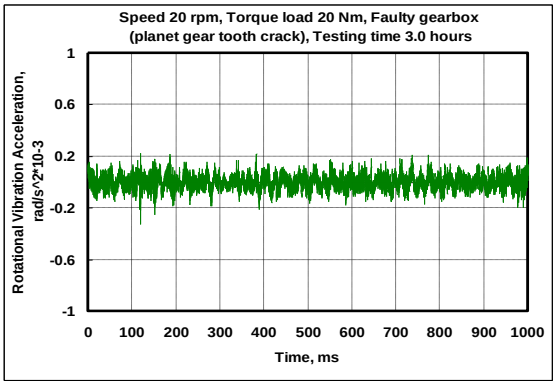

(a) Experimental time-domain signal at time of 3.0 h *h*

beta =1.2 scale =6

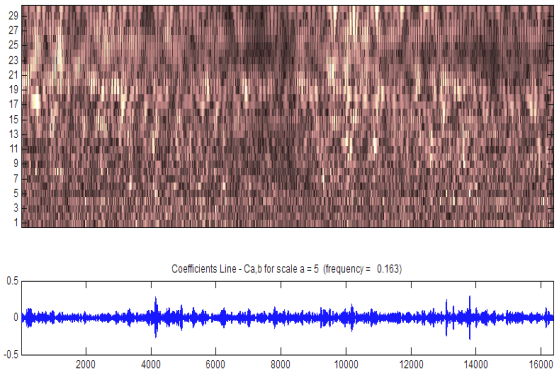

(b) Signal wavelet map at time of 3.0

Fig. 11 *Wavelet cracked planet gear of rotational vibration acc.(20 rpm, 20 Nm)*

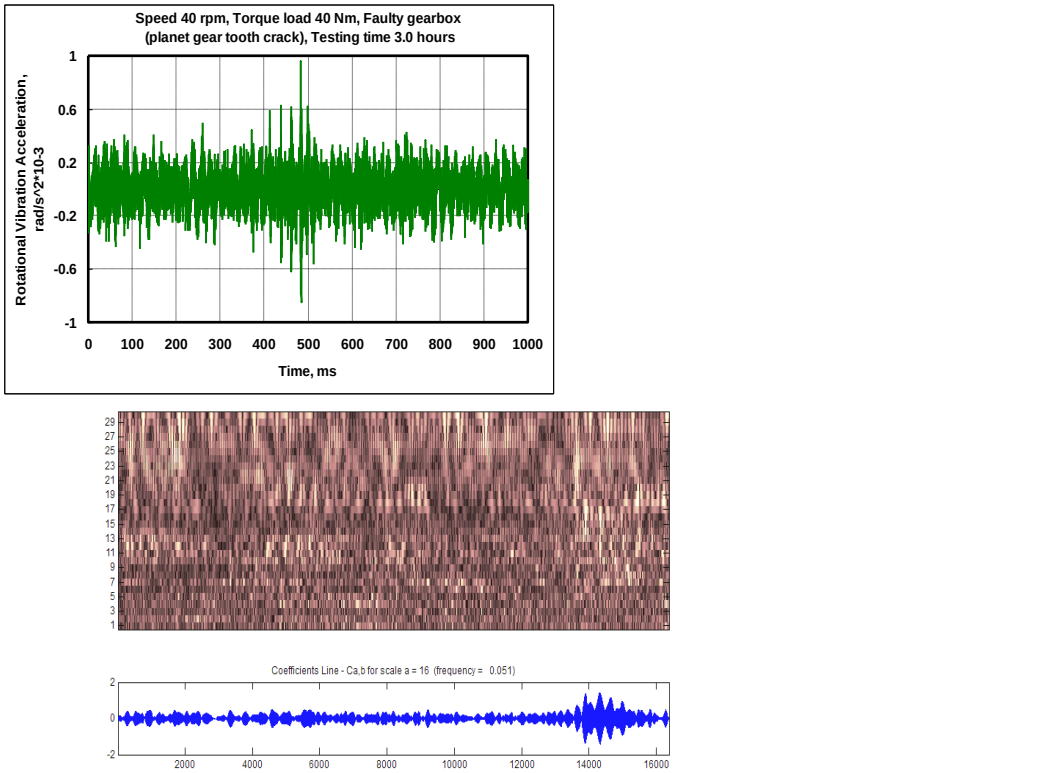

a) Experimental time-domain signal at time of 3.0 h b) *Signal wavelet map at time of 3.0 h beta =0.4 scale =8*

Fig. 12 *Wavelet cracked planet gear of rotational vibration acc. (40 rpm, 40Nm)*

Figures 13 and 14 show the computation of the correlated kurtosis (kurt) parameter for the filtered rotational vibration acceleration signals in terms of time-domain based on Equation (5) at speed 20 rpm and torque load 20 Nm; and at speed 40 rpm and torque load 40 Nm respectively with respect to testing time ranged from 0.0 min to 180 min. To assist the more accurate observation of this parameter computation during the range of testing time, a magnification was seen in the Figs. 13 (a) and 14 (a), where Figs.13 (b) and 14 (b) depict the averages of the change of kurtosis value for rotational vibration acceleration at 20 rpm, 20 Nm and at 40 rpm, 40 Nm from that of healthy gearbox components (CFHL) based on Equation (6) respectively.

Table 1 Average values of the change from the healthy Gearbox cracked planet gear

No	Speed rpm	Torque Nm	Average change from the healthy gearbox(CFHL), %	
			Transition 1	Transition 2
1	20	20	13.87	55.05
2	40	40	39.32	68.85

In Table 1 and at 20 rpm, 20 Nm, the first transition period which is obtained at the end of the testing time near 105 min, where CFHL is 13.87% while the second transition period is observed from 105 to 180 min and the averaged CFHL rise reaches 55.05%. At 40 rpm, 40 Nm, the first transition period which is obtained at the end of the testing time near 85 min, where CFHL is 39.32% while the second transition period is observed from 85 to 180 min and the averaged CFHL rise reaches 68.85%. These transition periods are important and possess diagnostic value, as they can be used to define and characterize critical changes of the planet gear tooth fault accumulation and evaluation. Furthermore, the results obtained will be helpful for determining the severity of planet gear tooth fault as well as remaining useful life prediction

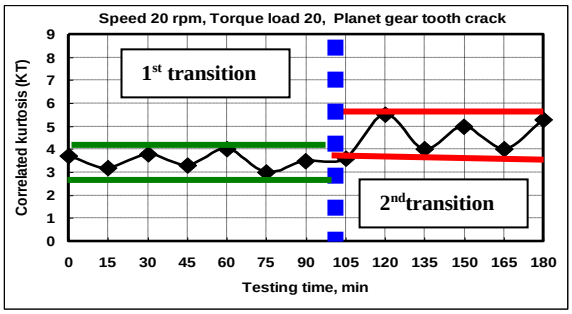

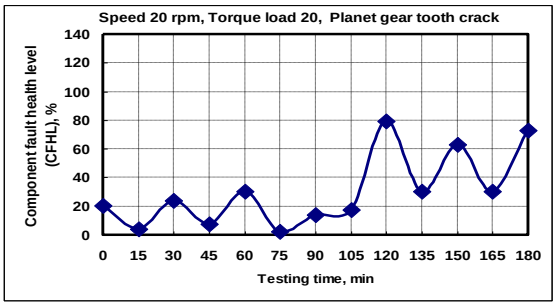

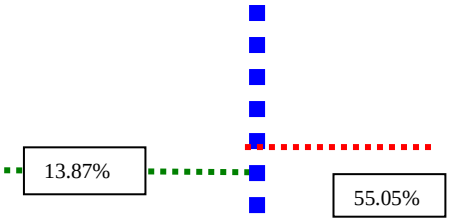

a) Kurtosis value - filtered rotational acceleration b) Change from the Healthy Gearbox (%)

Fig. 13 Wavelet filtered values at (20 rpm, 20 Nm) at testing time 3.0 h

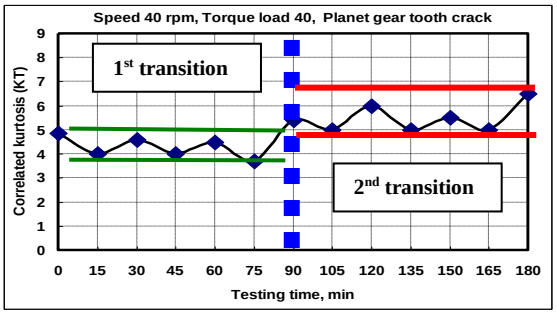

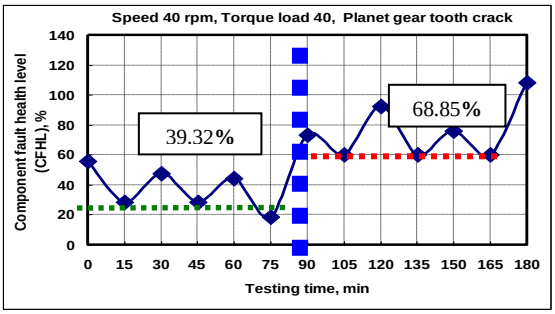

a) Kurtosis value - filtered rotational acceleration. b) Change from the Healthy Gearbox (%)

Fig.14Wavelet filtered values at(40 rpm, 40 Nm) at testing time 3.0 h

6.3. Spalling Planet GearSignal Analysis

Figures 15-16 depict the signal measured for faulty (spalling) planet gear tooth in terms of time-domain waveform at speed 20 rpm and torque load 20 Nm; and at speed 40 rpm and torque load 40 Nm respectively. Figs.15(a) and 16(a) show the experimental time domain signal at speed 20 rpm and torque load 20 Nm; and at speed 40 rpm and torque load 40 Nm respectively, while Figs.15(b) and 16(b) show the wavelet maps, where the distortion in color is nearly repeated each 600 (40 rpm 40 Nm) and 1200 (20 rpm, 20 Nm) samples. A close look at the vibration signal close to the gear meshing frequency reveals the presence of existing fault (spalling) in the gears of the gearbox. However, the spalling failure occurred near the pitch point, but the addendum surface did not fail and was smooth. When the driven gear meshes with the mating pinion, the tooth mesh starts from the addendum surface of the gear. The spalling dimensions are spalling length = 0.9 mm, spalling height = 1.0 mm and spalling width = 4.6 mm. The testing time is being 3.0 h.

Figures 17 and 18 show the computation of the kurtosis (kurt) parameter for the filtered rotational vibration acceleration signals in terms of time-domain based on Eq.(5) at speed 20 rpm and torque load 20 Nm; and at speed 40 rpm and torque load 40 Nm respectively with respect to testing time ranged from 0.0 min to 180 min. It is clear from the above figures that the kurtosis values are a sensitive and good indicator of gearbox faults at both different loads and speeds. On the other hand, the kurtosis does not indicate the magnitude of fault progress.

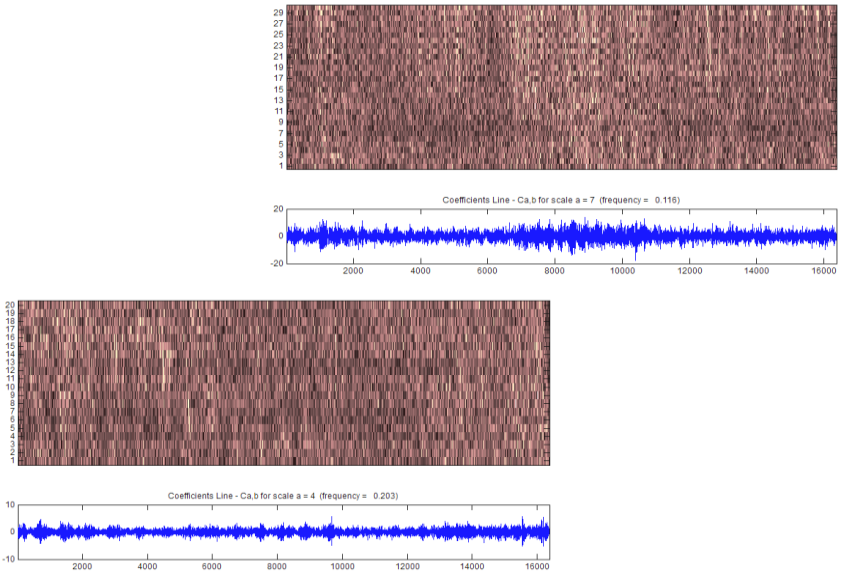

a) Experimental time-domain signal at time of 3.0 h beta =1.2 scale = 6 b) Signal wavelet map at time of 3.0 h

Fig. 15 Wavelet planet gear spalling of rotational vibration acc. (20 rpm, 20 Nm)

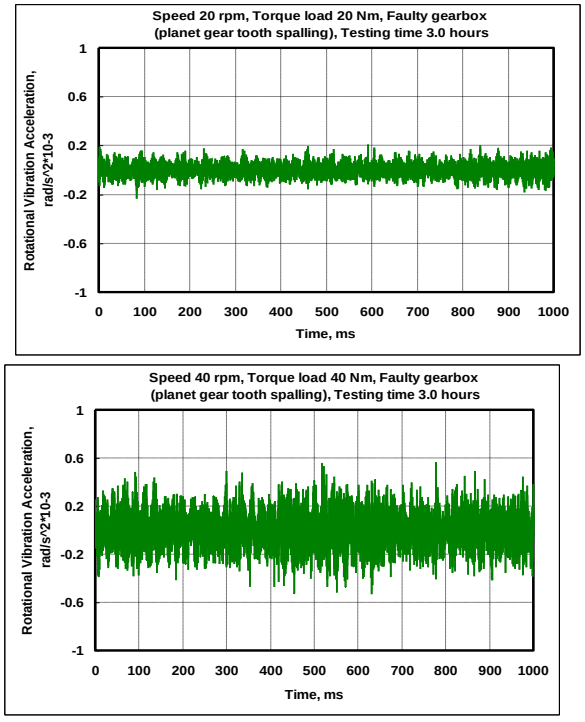

a) Experimental time-domain signal at time of 3.0 h b) Signal wavelet map at time of 3.0 h beta =1.2 scale = 8

Fig.16 Wavelet planet gear spalling of rotational vibration acc. (40 rpm, 40 Nm)

The kurtosis values are used as the best indicator of a fault at different loads because its values also indicate the fault progress, which may be useful for predictive maintenance, but it should be taken into consideration that it is not sensitive to speed. To assist the more accurate observation of this parameter computation during the range of testing time, a magnification was seen in the Figs. 17 (a) and 18 (a), while Figs. 17 (b) and 18 (b) depict the averages ofthe change of kurtosis value for rotational vibration acceleration at 20 rpm, 20 Nm and at 40 rpm, 40 Nm from that of healthy gearbox components (CFHL) based on Eq. (6) respectively.

Table 2 Average values of the change from the healthy gearbox to spalling planet gear

No	Speed rpm	Torque Nm	Average change from the healthy gearbox(CFHL), %	
			Transition 1	Transition 2
1	20	20	13.30	43.88
2	40	40	53.02	95.96

In Table 2 and at 20 rpm, 20 Nm, the first transition period which is obtained at the end of the testing time near 100 min, where CFHL is 13.30% while the second transition period is observed from 100 to 180 min and the averaged CFHL rise reaches 43.88%. At 40 rpm, 40 Nm, the first transition period which is obtained at the end of the testing time near 90 min, where CFHL is 53.02% while the second transition period is observed from 90 to 180 min and the averaged CFHL rise reaches 95.96%. These transition periods are important and possess diagnostic value, as they can be used to define and characterize critical changes of the planet gear tooth fault accumulation and evaluation. It is clear that fault detection and classification (faulty gear) can be achieved using vibration analysis. Kurtosis is a parameter that is sensitive to the signal peaks and is well adapted to the impulse nature of the simulating forces generated by component damage. Over time the defect becomes greater or more defects propagate in the gearbox in such manner that the impulsive signal changes to a continuous one Furthermore, the results obtained will be helpful for determining the severity of planet gear tooth fault as well as remaining useful life prediction.

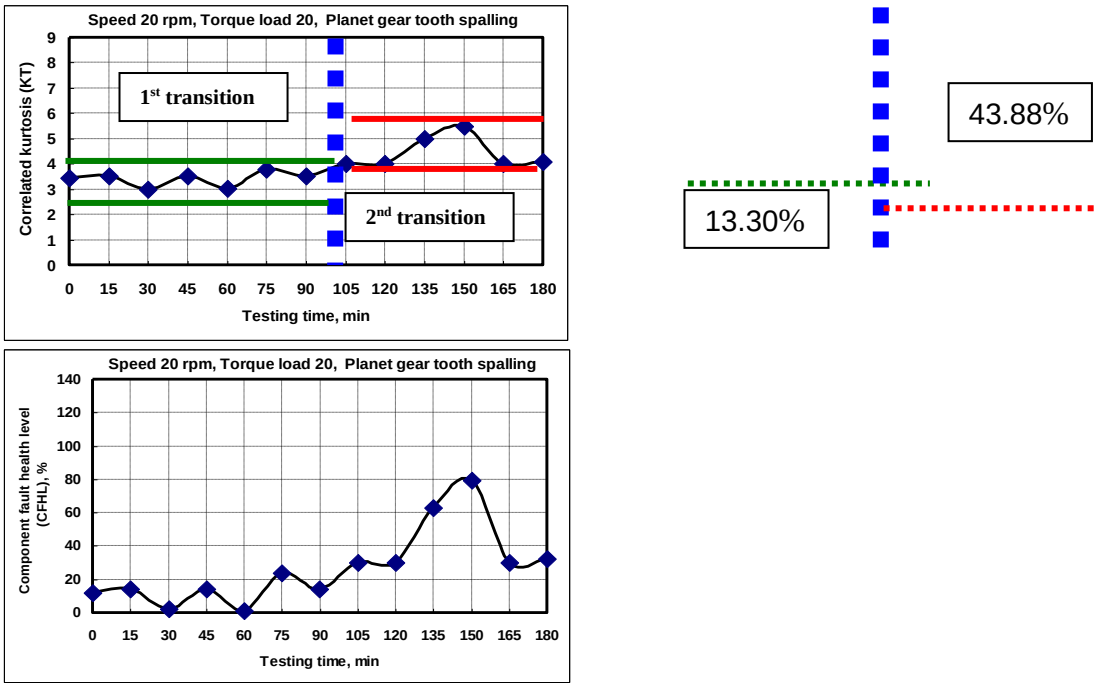

a) Kurtosis value - filtered rotational acceleration b) Change from the Healthy Gearbox (%)

Fig. 17Wavelet filtered values at (20 rpm, 20 Nm) at testing time 3.0 h

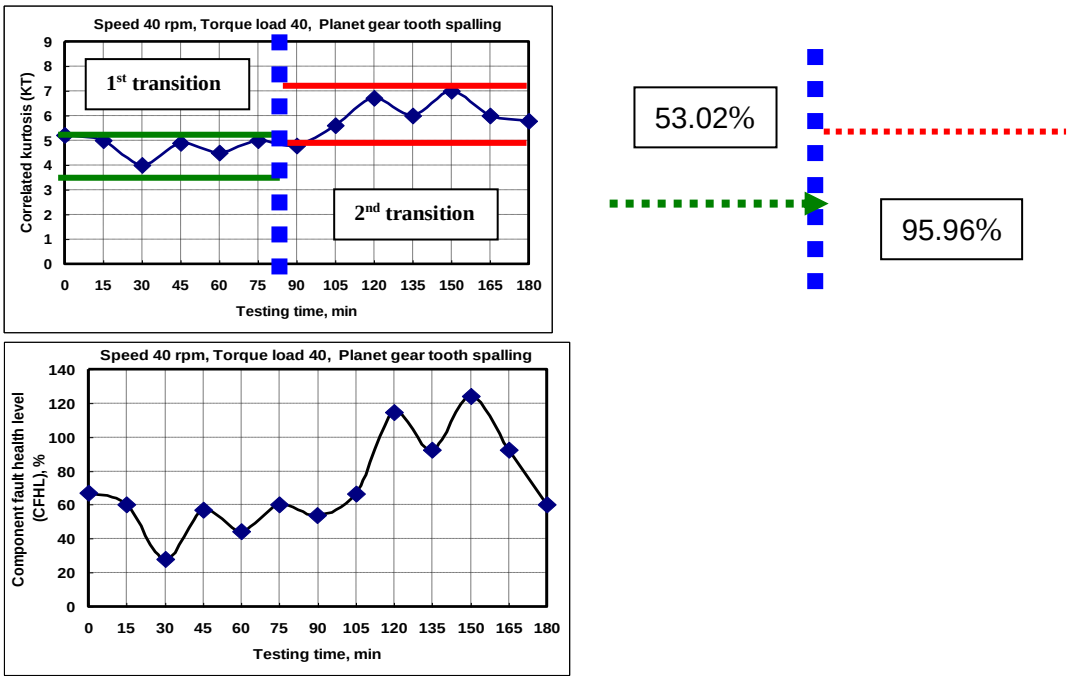

a) Kurtosis value - filtered rotational acceleration b) Change from the Healthy Gearbox (%)

Fig. 18Wavelet filtered values at (40 rpm, 40 Nm) at testing time 3.0 h

6.4 Breakage Planet Gear Signal Analysis

Figures 19 and 20 depict the signal measured for faulty (breakage) planet gear tooth in terms of time-domain waveform at speed 20 rpm and torque load 20 Nm; and at speed 40 rpm and torque load 40 Nm respectively.. Figs.19(a) and 20(a) show the experimental time domain signal at speed 20 rpm and torque load 20 Nm; and at speed 40 rpm and torque load 40 Nm respectively, while Figs.19(b) and 20(b) show the wavelet maps, where the distorsion in color is nearly repeated each 600 (40 rpm 40 Nm) and 1200 (20 rpm, 20 Nm) samples. A close look at the filtered vibration signal close to the gear meshing frequency, one can observe that some absolute maximum points show the position of breakage fault in planet gear. These figures also show that wavelet filtering alone is unable to extract periodic features properly and no periodic impulses appear on any scale in either wavelet scales. It is inferred that CWT alone, is not effective in detecting faults in the gearboxes. Presence of periodical impulses in noisy gear signals often indicates the occurrence of fault symptoms. The extraction of impulsive features in noisy gear signals is vital in process of gear fault diagnosis. The breakage dimensions are breakage thickness = 0.6 mm, breakage width=4.6 mm and breakage height=1.35 mm. The testing time is being 3.0 h.

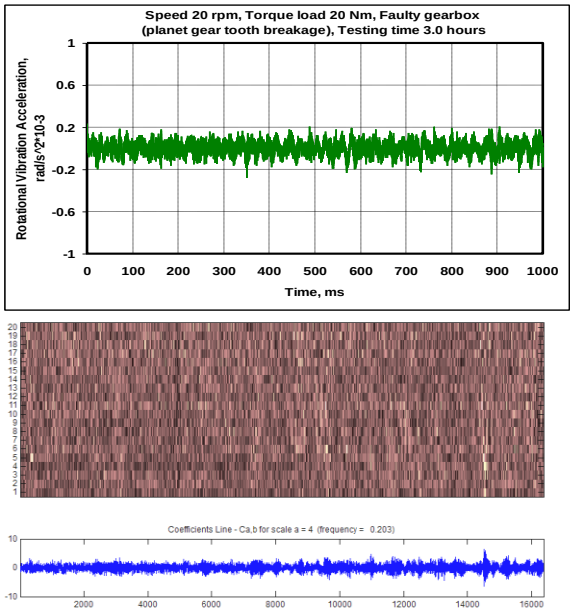

a) Experimental time-domain signal at time of 3.0 h *b) Signal wavelet map at time of 3.0 h*

Fig.19Wavelet planet gear breakage of rotational vibration acc.(20 rpm, 20 Nm)

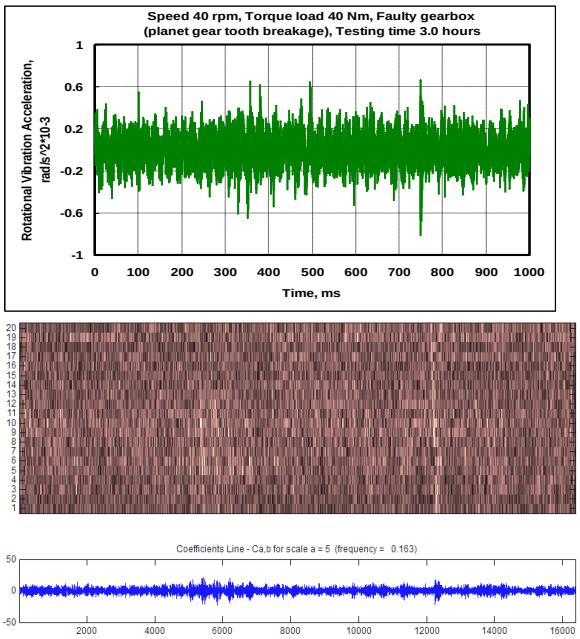

a) Experimental time-domain signal at time of 3.0 h b) Signal wavelet map at time of 3.0 h

Fig.20 Wavelet planet gear breakage of rotational vibration acc. (40 rpm, 40 Nm)

Figures 21 and 22 show the computation of the kurtosis (kurt) parameter for the filtered rotational vibration acceleration signals in terms of time-domain based on Eq. (5) at speed 20 rpm and torque load 20 Nm and at speed 40 rpm and torque load 40 Nm respectively with respect to testing time ranged from 0.0 min to 180 min. To assist the more accurate observation of this parameter computation during the range of testing time, a magnification was seen in the Figures 21 (a) and 22 (a), where Figures21 (b) and 22 (b) depict the averages of the change of kurtosis value for rotational vibration acceleration at 20 rpm, 20 Nm and at 40 rpm, 40 Nm from that of healthy gearbox components (CFHL) based on Eq. (6) respectively

Table 3 Average values of the change from the healthy gearbox to breakage planet gear

No	Speed rpm	Torque Nm	Average change from the healthy gearbox (CFHL) %	
			Transition 1	Transition 2
1	20	20	20.96	69.50
2	40	40	36.26	73.42

A magnification is obtained, and it is important and possesses better diagnostic value as they can be used to define and characterize critical changes of the gear's faults accumulation and evaluation. However, the change around the kurtosis number indicates higher deterioration than that recorded in the case of the stationary signal.

In Table 3 and at 20 rpm, 20 Nm, the first transition period which is obtained at the end of the testing time near 100 min, where CFHL is 20.96%, while the second transition period is observed from 100 to 180 min and the averaged CFHL rise reaches 69.50%. At 40 rpm, 40 Nm, the first transition period which is obtained at the end of the testing time near 75 min, where CFHL is 36.26%, while the second transition period is observed from 75 to 180 min and the averaged CFHL rise reaches 73.42%. These transition periods are important and possess diagnostic value, as they can be used to define and characterize critical changes of the planet gear tooth fault accumulation and evaluation. Furthermore, the results obtained will be helpful for determining the severity of planet gear tooth fault as well as remaining useful life prediction

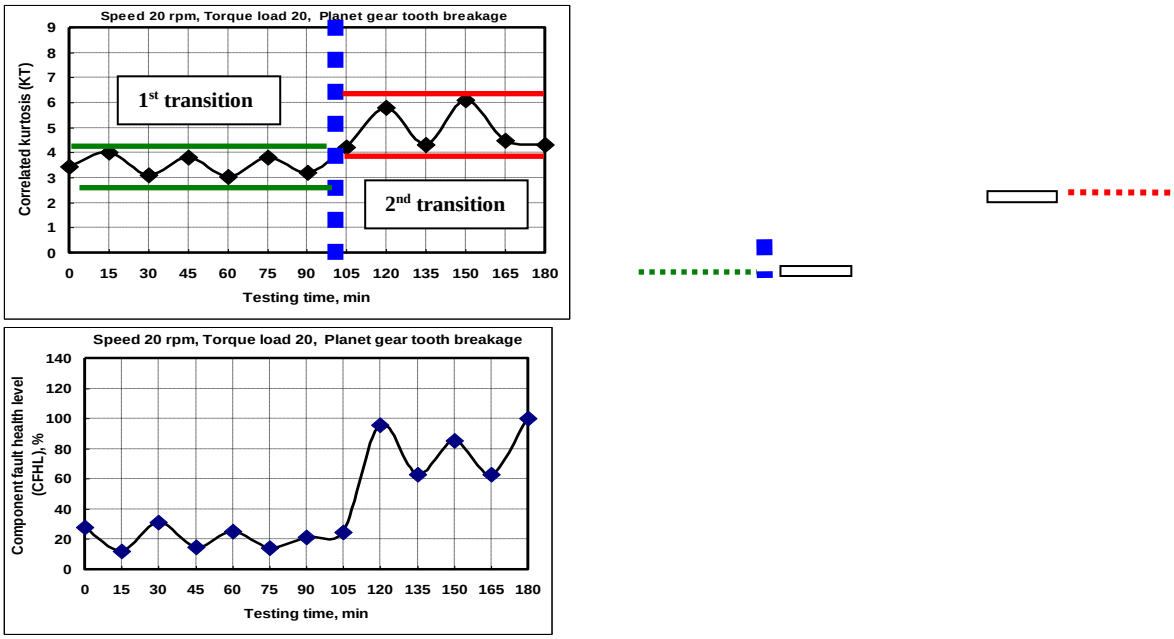

a) Kurtosis value - filtered rotational acceleration b) Change from the Healthy Gearbox (%)

Fig. 21 Wavelet filtered values at (20 rpm, 20 Nm) at testing time 3.0 h

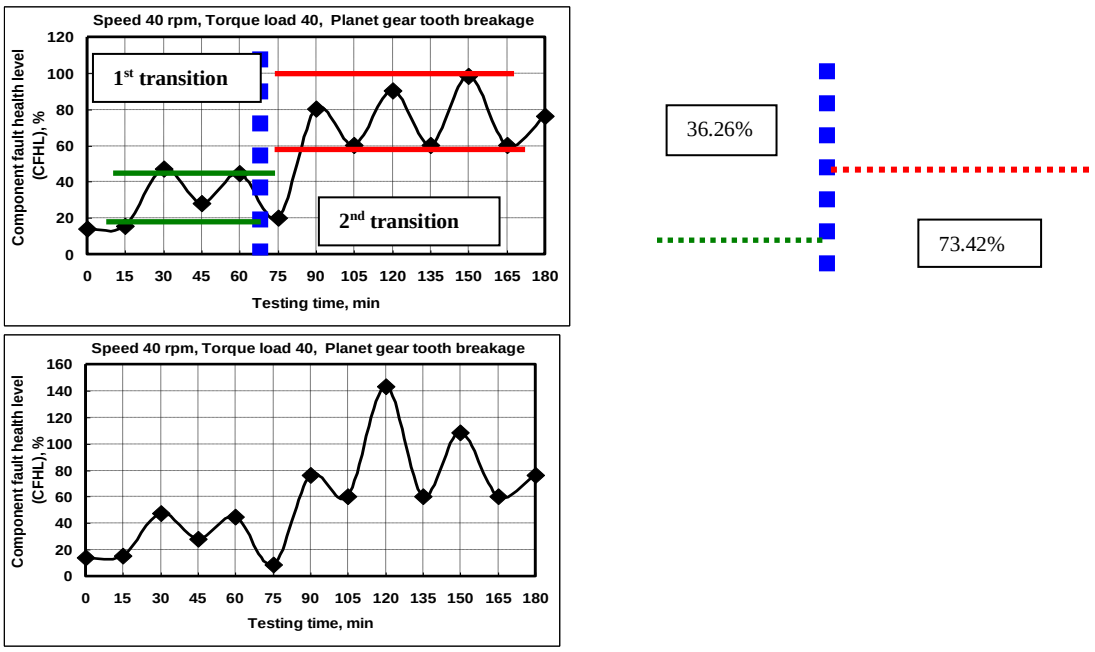

a) Kurtosis value - filtered rotational acceleration b) Change from the Healthy Gearbox (%)

Figure 22 Wavelet filtered values at (40 rpm, 40 Nm) at testing time 3.0 h

7. Conclusion

It has been shown that the faults on wind turbine planetary gear box can be detected at its early stages, and symptoms of fault on vibration is not primarily caused by the reduction components stiffness (which is the case for the detection of a localized fault), but mainly due to the deviations in component shape from the true component shape.

The wind turbine planetary gearbox was utilized in order to study the development of fault in artificially induced crack, spall and break in planet gear tooth. Multi-hour tests were conducted.
and numerous recording were acquired using vibration monitoring. The kurtosis parameter (indicator) is proposed. Among it, conventional time domain based kurtosis parameter and a set of innovative kurtosis parameter based on the Morlet wavelet transform.

Transitions in the kurtosis values were highlighted suggesting critical changes in the operation of the gearbox. Moreover, these transition periods are important and possess diagnostic value, as they can be used to define and characterize critical changes of the planet gear tooth fault accumulation and evaluation. Furthermore, the results obtained will be helpful for determining the severity of planet gear tooth fault as well as remaining useful life prediction

In non-stationary vibration waveform features and in the process of feature extraction, it is required that the timescale structure of a wavelet should be consistent with the feature components. For a Morlet, its time and frequency resolution can be altered by adjusting the value of the shape of the daughter (β). The Morlet wavelet can be used for impulse detection due to its similarity to an impulse. Any wavelet can be viewed as a filter. To identify impulses hidden in noisy signals by filtering, the wavelet should well match the time-frequency structure of the impulse. An adaptive Morlet wavelet filter based on the kurtosis maximization is proposed to detect periodic impulses automatically for recognition of gear tooth crack.

Acknowledgement

This research did not receive any specific grant from funding agencies in the public, commercial, or not-for-profit sectors.

References

Abouel-seoud, S. A. 2018. Fault detection enhancement in wind turbine planetary gearbox via stationary vibration waveform data" Journal of Low Frequency Noise, Vibration and Active Control, Vol. 37(3) 477–494

Chen, J., Li, G. and Racic, V. 2018. A data-driven wavelet-based approach for generating jumping loads Mechanical Systems and Signal Processing June 2018; Volume 106: 49-61

Chen, J., Zi, Y., He, Z. and Yuan, J. 2013 .Compound faults detection of rotating machinery using improved adaptive redundant lifting multiwavelet. Mechanical Systems and Signal Processing July 2013; Volume 38: Issue 1: 36-54

Cui, H, Qiao,Y., Yin Y. and Hong, M. 2017. An investigation on early bearing fault diagnosis based on wavelet transform and sparse component analysis Structural Health Monitoring; Vol. 16(1): 39–49

Entezami, A. and Shariatmadar, H. 2018. Damage localization under ambient excitations and non-stationary vibration signals by a new hybrid algorithm for feature extraction and multivariate distance correlation methods. Structural Health Monitoring; 4(2): 1–29.

Ewins, J. 1986. Modal Testing: Theory and Practice. Research Studies Press LTD1986;BRUEL.& KJÆR.

Gorgei, P., Sertbas, A., Kilic, N., Ucan, O. N. and Osman O.2009.Mammo-graphic Mass Classification Using Wavelet Based Support Vector Machine Istanbul University. Journal of Electrical & Electronics Engineering; Vol. 9: No. 1: 867-875

Iatsenko, D., McClintock, P.V.E. and Stefanovska, A.2013. Extraction of instantaneous frequencies from ridges in time-frequency representations of the signals Signal Processing; Volume 125: 290-303.

Kaltungo, A , Sinha, J. and Nembhard, A. 2015. A novel fault diagnosis technique for enhancing maintenance and reliability of rotating machines. Structural Health Monitoring Vol. 14(6): 604–621

Lei, Y., Han, D, Lin, J. and He, Z. 2013 .Planetary gearbox fault diagnosis using an adaptive stochastic resonance method. Mechanical Systems and Signal Processing July 2013; Volume 38: Issue 1: 113-124

Li, P. and Xiang, J. 2014 .Fault Diagnosis of Gearbox in Wind turbine Based on Wavelet Transform and Support Vector Machine. Applied Mechanics and Materials; Vols 536-537: 18-21

Márquez, F.P.G., Tobias, A.M. and Pérez, J.M.P 2012 .Condition monitoring of wind turbines: Techniques and methods. Renewable Energy, 46: 169-178.

Morsy, M., Abouel-seoud, S. and Rabeih, M. Sept,2010. Geared system condition diagnostics via torsional vibration measurement. ISMA; International Conference onNoise and Vibration.

Morsy, M., Abouel-seoud, S. and Rabeih, M. 2011. Gearbox damage diagnosis using wavelet transform technique. International Journal of Acoustics and Vibration; Vol. 16: No. 4, 173-179.

Musial, W., Butterfield, S. and McNiff, B. 2007.Improving wind turbine gearbox reliability. European Wind Energy Conference, Milan, Italy: May 7–10**.**

Sharma V and Parey A 2015.Fault diagnosis of gearbox using various condition monitoring indicators for nonstationary speed conditions: A Comparative Analysis. 2nd International and 17th National Conferences on Machines and Mechanisms;iNaCoMM20: 15-13

Stiesdal, H. 1999. The wind turbine components and operation. Special Issue, Bonus INFO1999, Autumn.